Journal of proteome research

pubs.acs.org/jpr

Article

Expanding Targeted Instrumentation for Discovery Applications: Complement Reporter Ion Quantification with a Quadrupole–Ion Trap Instrument

Edward R. Cruz, Alex N. T. Johnson, Vyas Pujari, Qi Zhang, Thao Nguyen, Michael Stadlmeier, Jessica Wang, Cristina C. Jacob, Graeme C. McAlister, Philip M. Remes,* and Martin Wühr*

Cite This: https://doi.org/10.1021/acs.jproteome.5c00356

Read Online

ACCESS | Metrics & More | Article Recommendations | Supporting Information

ABSTRACT: Proteomic workflows have traditionally been divided into discovery-based and targeted approaches with instrumentation optimized specifically for each. Discovery experiments typically utilize high-resolution analyzers, while targeted workflows rely on the sensitivity and specificity of triple quadrupole systems. Recently, a quadrupole–ion trap instrument (Stellar MS) has demonstrated superior performance for targeted applications compared to conventional triple quadrupoles. In this study, we expand the capabilities of this platform to multiplexed shotgun proteomics using complement reporter ion quantification in an ion trap (iTMTproC). Benchmarking experiments with defined standards show that iTMTproC achieves quantification accuracy and interference reduction comparable to MultiNotch MS^3 on the Orbitrap Fusion Lumos, a dedicated quadrupole–ion trap–Orbitrap tribrid instrument optimized for this purpose. Notably, iTMTproC quantifies slightly more proteins than does MultiNotch MS^3. We further validate this approach through a developmental time-series analysis of frog embryos, obtaining proteomic data nearly indistinguishable from those from MultiNotch MS^3, with slightly increased protein quantification depth. These findings significantly extend the functionality of targeted instrumentation, underscoring the versatility of quadrupole–ion trap systems and providing cost-effective access to highly accurate, multiplexed quantitative shotgun proteomics.

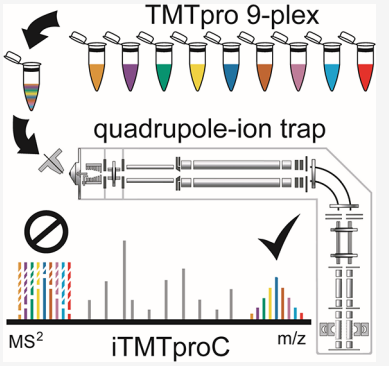

KEYWORDS: *quadrupole–ion trap, multiplexing, shotgun proteomics, complement reporter ions, Stellar, TMTpro*

INTRODUCTION

Proteomic experiments traditionally follow two distinct paradigms: discovery-based (shotgun) approaches and targeted analyses.[1−4] Discovery proteomics aims to identify and quantify thousands of proteins in complex samples, typically using high-resolution mass analyzers capable of resolving and identifying diverse peptide populations in an unbiased manner.[5,6] In contrast, targeted proteomics measures predefined subsets of proteins or peptides, achieving higher quantitative precision and reproducibility across multiple samples.[1,2,7] Classic targeted workflows often utilize triple quadrupole or quadrupole–ion trap instruments for selected or multiple reaction monitoring (SRM/MRM), enabling rapid, sensitive measurements at nominal mass resolution.[8−10] Recently, a quadrupole–ion trap mass spectrometer (Stellar MS) demonstrated superior performance in targeted workflows compared to conventional triple quadrupole instruments, achieving a 10-fold improvement in limits of quantitation and a 2-fold improvement in detection limits[11] (Figure 1a,b).

Among discovery-based proteomic techniques, two leading strategies are data independent acquisition (DIA) and multiplexed proteomics based on isobaric tagging.[12−16] Isobaric mass tags, such as TMTpro, enable the simultaneous quantification of peptides from multiple samples within a single experiment.[17,18] This multiplexing approach substantially boosts throughput and experimental consistency by eliminating inter-run variability. However, early MS^2-based implementations of multiplexing face a key obstacle: reporter ion ratio distortion caused by coisolated peptides, which leads to inaccurate quantification.[19−21] To mitigate interference, MS^3-based methods were introduced, utilizing an additional fragmentation step (MultiNotch MS^3) to coisolate and fragment b- and y-ions specifically related to the targeted peptide[19,22] (Figure 1c,d). While this MS^3 strategy substantially reduces ratio distortion and enhances quantification accuracy, it sacrifices acquisition speed and requires specialized hybrid mass spectrometers, i.e., tribrid quadrupole–ion trap–Orbitrap instruments. Recent advancements incorporate real-time search (RTS) capabilities with MultiNotch MS^3, allowing MS^3 scans to be selectively triggered only

Received: April 16, 2025
Revised: June 25, 2025
Accepted: July 25, 2025

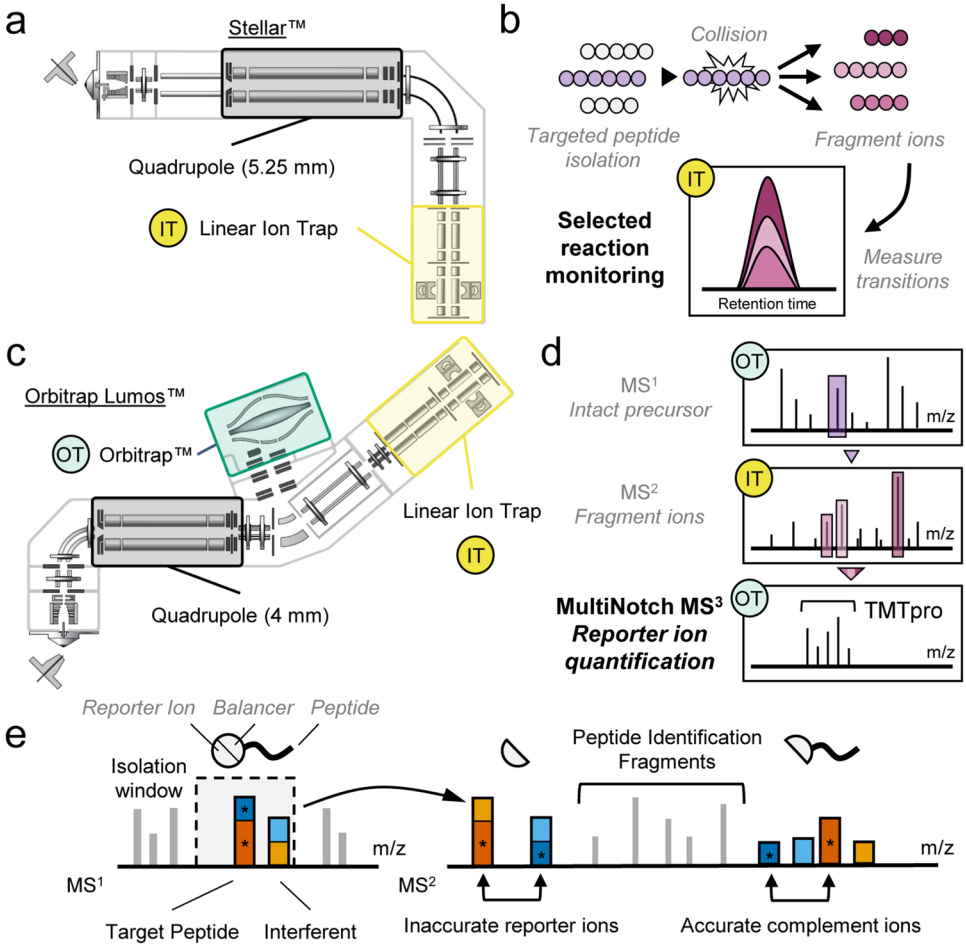

Figure 1. Comparison of Orbitrap Lumos and Stellar and their primary intended usage. (a) Schematic of the Stellar. The Stellar is optimized for high-sensitivity targeted applications, incorporating a linear ion trap and a state-of-the-art quadrupole (field radius of 5.25 mm), which surpasses the quadrupole used in the Orbitrap Lumos (field radius of 4 mm). Analyzers shared with the Orbitrap Lumos are colored black and yellow. In later subpanels, the Orbitrap is highlighted in green, and in the example workflows, OT (Orbitrap) and IT (ion trap) indicate which analyzer performs the corresponding scan. (b) Targeted proteomics on the Stellar. The Stellar is tailored for targeted workflows, such as selected reaction monitoring (SRM), in which peptides of interest are selectively isolated, fragmented, and their fragment ions ("transitions") are monitored for quantitative analysis. (c) Schematic of the Orbitrap Lumos. The Orbitrap Lumos is a tribrid mass spectrometer designed to support accurate multiplexed shotgun proteomics using MultiNotch MS^3. It integrates three mass analyzers: a quadrupole, an Orbitrap, and a linear ion trap. (d) Workflow of MultiNotch MS^3 multiplexed shotgun proteomics on the Orbitrap Lumos. In MultiNotch MS^3 using TMTpro reagents, synchronous precursor selection (SPS) is employed to isolate multiple fragment ions from the MS^2 scan simultaneously. These selected ions are further fragmented in a MS^3 scan to generate reporter ions for quantification. This additional fragmentation step reduces interference from coisolated peptides, thereby improving quantification accuracy in complex samples. (e) Principle of complement reporter ion quantification (TMTproC). During MS^1 isolation, the isolation window captures both the target peptide (dark orange and blue) and coisolated interfering peptides (light orange and blue). In conventional MS^2-based workflows, these coisolated peptides produce indistinguishable reporter ions, leading to quantification errors. TMTproC addresses this by leveraging complement ions, which retain the intact peptide backbone, along with the balancer group. Because this balancer−peptide conjugate encodes both peptide identity and sample origin, TMTproC reduces interference from unrelated peptides and enables more accurate quantification.

upon successful peptide identification during MS^2 analysis.[23,24] This innovation further enhances measurement accuracy by exclusively isolating b- and y-ions carrying isobaric tags from peptides of interest.[24]

An alternative strategy for accurate multiplexed quantification at the MS^2 level, known as TMTproC, utilizes complementary reporter ions.[25−28] Unlike traditional low-mass reporter ion quantification, TMTproC leverages balancer-group fragment ions that retain isotopic label information in the mid- to high-mass region. Because complementary ion masses are precursor-specific, they substantially reduce coisolation interference (Figure 1e). To date, TMTproC methods have been implemented entirely on high-resolution mass analyzers, whose precision and resolving power reliably distinguish complementary ion clusters from background signals. Compared to conventional MS^3 quantification, a key limitation of TMTproC is its reduced multiplexing capacity: in most routine applications, only 9 of the 18 available TMTpro tags can be resolved.[28] This limitation, though, is not fixed; super-resolution techniques now enable the use of shorter transients combined with postacquisition processing to achieve effective resolving powers of ≥500 K, allowing extension to a 12-plex TMTproC setup without ultralong transient acquisition.[29] Although this limited channel count reduces throughput compared to modern Orbitrap-based TMT workflows, which now support up to 35-plex with differential elution[30] (or up to 18-plex without deuterium incorporation), TMTproC remains attractive for

https://doi.org/10.1021/acs.jproteome.5c00356
J. Proteome Res. XXXX, XXX, XXX−XXX

settings where cost and instrument accessibility are primary concerns.

Continued advances like super-resolution have expanded the multiplexing capabilities of high-end instrumentation, but it remains equally important to facilitate broader adoption of accessible and affordable mass spectrometers. Therefore, we explored the feasibility of adapting TMTproC methods to lower-resolution analyzers, specifically a quadrupole−ion trap instrument, to increase their utility in discovery-based proteomics.

Herein, we introduce iTMTproC—an adaptation of TMTproC for quadrupole−ion trap instrumentation—enabling nine-channel multiplexed peptide quantification on a cost-effective, low-resolution platform. We benchmarked iTMTproC against established multiplexed quantification methods, demonstrating comparable accuracy and sensitivity to MultiNotch MS^3 workflows on Orbitrap Lumos. Although data quality and sensitivity do not match specialized multiplexing approaches like RTS-MS^3 and RTS-TMTproC,[24,28] our development represents a critical step toward democratizing multiplexed shotgun proteomics in laboratories lacking access to high-end mass spectrometry.

EXPERIMENTAL PROCEDURES

Proteomic Sample Preparation

Proteomic samples were prepared as previously described.[27,31,32] In brief, following cell lysis, samples were reduced with 5 mM dithiothreitol (DTT) for 20 min at 60 °C and alkylated with 20 mM *N*-ethylmaleimide for 20 min at room temperature. 5 mM DTT was added to quench the excessive alkylating reagents. Proteins were purified using one of the following two methods, depending on the sample: (1) For our HeLa and yeast samples, proteins were purified by methanol−chloroform precipitation,[33] and the resulting dried pellet was resuspended in 10 mM *N*-(2-hydroxyethyl)piperazine-*N*′-3-propanesulfonic acid (EPPS; pH 8.5) with 6 M guanidine hydrochloride. Samples were heated at 60 °C for 15 min, and the protein mixture was diluted 3-fold with 10 mM EPPS (pH 8.5). (2) For our *Xenopus laevis* samples, proteins were precipitated following reduction and alkylation using the SP3 method, as previously described.[34] After binding and washing the bead-bound protein, the protein-containing beads were resuspended in 2 M guanidine hydrochloride. Following protein precipitation, the protein mixture was digested with 20 ng/μL LysC (Wako) overnight at room temperature. Samples were further diluted 4-fold with 10 mM EPPS (pH 8.5) and digested with an additional 20 ng/μL LysC and 10 ng/μL sequencing-grade trypsin (Promega) at 37 °C for 16 h. After digestion, the peptides were cleared by ultracentrifugation at 100000*g* for 1 h at 4 °C, and the supernatant was vacuum-dried. For TMTpro labeling, TMTpro tags were added at a ratio of 5 μg of TMTpro/1 μg of peptide, mixed, and incubated at room temperature for 2 h. The reaction was then quenched by addition of 5 μL of 5% hydroxylamine at room temperature for 30 min. The resulting mixture was vacuum-dried, desalted using homemade stage tips with C18 material (Empore), and resuspended in 1% formic acid to 1 μg/μL before LC−MS analysis.

For the *Xenopus* development time course, prefractionation was utilized to detect a larger number of peptides.[35] Specifically, before LC−MS analysis, the dried peptides were resuspended in 10 mM ammonium bicarbonate (pH 8) with 5% acetonitrile to a peptide concentration of 1 μg/μL. The dissolved peptides were separated into 96 fractions using medium-pH reverse-phase separation (Zorbax 300Extend C18, 4.6 × 250 mm^2 column) on a 1260 Infinity II LC system (Agilent), as described previously.[35] Each resulting 96-well plate was combined into 24 fractions, and each fraction was desalted and resuspended for LC−MS analysis, as described above.

HeLa−Yeast Interference Standard

HeLa S3 cells were grown on 10 cm tissue culture plates to 80% confluency, and *S. cerevisiae* S288C was grown to an OD of 0.4 in YPD as a suspension culture. HeLa cells were pelleted and lysed by sonication in 100 mM HEPES buffer (pH 7.2) with 2% SDS and a Roche protease inhibitor. Yeast cells were lysed by cryomilling and later resuspended in 50 mM HEPES (pH 7.2) with 4% SDS and 1 mM DTT. Samples were further prepared as described above. For TMTpro labeling, yeast lysate was labeled at 0:1:5:10:1:10:5:1:0 ratios using the nine TMTproC-compatible channels, and the HeLa lysate was labeled as 1:1 using the same channels. Prior to desalting, the TMT-labeled yeast and HeLa lysate were mixed with HeLa/yeast at a 10:1 ratio.

Collection of Developing *Xenopus laevis* Embryos

Mature *X. laevis* females and males were purchased from Xenopus1 and maintained by the Laboratory Animal Resources at Princeton University. All animal procedures were approved under Institutional Animal Care and Use Committee protocol 2070. Unfertilized eggs and male testes were collected following standard laboratory procedures described previously.[36] For testes collection, *X. laevis* males were euthanized in 0.1% (w/v) tricaine methanesulfonate (MS-222; Syndel's Syncaine) and then sacrificed by pithing. The testes were isolated and stored at 4 °C in oocyte culture medium [1 L/13.7 g Leibovitz's L-15 medium powder (Thermo Fisher Scientific; #41300039), 8.3 mL penicillin−streptomycin (Thermo Fisher Scientific; #15140122), and 0.67 g bovine serum albumin], which was changed daily for up to 1 week. For egg collection, female frogs were injected with 500 U of human chorionic gonadotropin (CG10; Sigma) and kept at 16 °C in Marc's modified Ringer's solution for 16 h before collection (1× MMR: 5 mM HEPES (pH 7.8), 0.1 mM EDTA, 100 mM NaCl, 2 mM KCl, 1 mM $MgCl_2$, and 2 mM $CaCl_2$). For *in vitro* fertilization, female eggs collected in 1× MMR buffer were cleaned, and preactivated eggs were removed. Half of one male testis was used per 500 eggs by crushing them in 1× MMR buffer with a sterile pestle and then mixing them with unfertilized eggs. The mixture was incubated at 16 °C for 5 min, followed by mixing and additional 5 min of incubation. Fertilization was induced by flooding the eggs with 0.1× MMR. After 1 h at 16 °C, embryo jelly coats were removed by incubating with 2% cysteine in 0.1× MMR for 5 min, and the embryos were thoroughly washed with 0.1× MMR to remove residual cysteine. Embryos were grown and staged according to the Nieuwkoop and Faber[37] nomenclature at 16 °C and then flash-frozen at desired time points. Embryo lysis was performed as described previously[31] and following the sample preparation protocol stated above.

UHPLC Chromatography

All proteomic samples were analyzed on a Vanquish Neo UHPLC system or a Proxeon 1200. Solvent A consisted of 2% DMSO and 0.125% formic acid in water, and solvent B consisted of 80% acetonitrile, 2% DMSO, and 0.125% formic acid in water. Depending on the experiment, the UHPLC system was coupled to an Ascend (Vanquish), an Orbitrap Lumos (Proxeon), or a

https://doi.org/10.1021/acs.jproteome.5c00356
J. Proteome Res. XXXX, XXX, XXX−XXX

Stellar (Vanquish) mass spectrometer. Notably, Orbitrap Lumos and Stellar utilized entirely separate UHPLC systems at two distinct locations. On all instruments, peptides were separated on an Aurora Series emitter column (25 cm × 75 μm inner diameter, 1.6 μm C18; IonOpticks) and were held at 60 °C using an in-house-built column oven, while experiments with the Stellar utilized a Nanospray Flex ion source (Thermo Fisher).

All samples were analyzed with the following 90 min gradient at a constant flow rate of 350 nL/min after thorough equilibration of the column to 0% B: 0−10% B in 5 min, 10−26.4% B for 70 min, 26.4−100% for 10 min, and 100% for 5 min. For electrospray ionization, 2.6 kV was applied between 1 and 83 min of the LC gradient. To avoid carryover of peptides, 2,2,2-trifluoroethanol was injected in a 30 min wash between each sample.[38] For fractionated samples, this wash was performed between every three fractions from the same original sample.

Ion-Trap Complement Reporter Ion Quantification Method

iTMTproC optimization experiments were performed on the Ascend. The instrument designation based on the experiment is as follows: optimization of iTMTproC parameters − Ascend (Figures 2, S2, and S3), interference standard comparison with a MultiNotch MS^3 − Stellar (Figure 3), and *Xenopus* developmental proteomics − Ascend (Figure 4).

The mass spectrometer was set to analyze positively charged ions in data-dependent MS^2 mode, recording centroid data with the RF lens level at 60%. Full scans were taken with the ion trap at 33 kDa/s (normal resolution) with an automatic gain control (AGC) target of 3×10^4 ions, maximum IIT of 30 ms, and scan range of 500−1200 m/z with wide quadrupole isolation enabled. The maximum cycle time between MS1 scans was set to 3 s.

Following the survey scan, the following filters were applied for triggering the MS^2 scans. Isolated masses were excluded for 15 s after triggering a mass tolerance window of ±0.5 m/z. Ions were analyzed if their m/z ratio was between 550 and 1050 to ensure visibility of the complementary ion clusters in a normal-range MS^2 scan. An intensity threshold was set for 5×10^3 ions.

The following settings were used for ion-trap MS^2 scans. The AGC target was set to 7.5×10^4 charges, and the maximum IIT was 50 ms. The quadrupole was utilized for isolation with an isolation width of 0.4 Da, and ions were fragmented with collision induced dissociation (CID) at a normalized collision energy of 35% (10 ms activation time and 0.25 activation Q). The scan rate was set to 33 kDa/s (normal resolution) in autoscan range mode with a default charge state of 2.

MultiNotch MS^3 Method

MultiNotch MS^3 experiments were performed on the Orbitrap Lumos and Ascend. The instrument designation based on experiment is as follows: interference standard comparison with iTMTproC − Orbitrap Lumos (Figure 3), interference standard comparison with iTMTproC − Ascend (Figure S4), and *Xenopus* developmental proteomics − Ascend (Figure 4).

The mass spectrometer was set to analyze positively charged ions in data-dependent MS^3 mode, recording centroid data with the RF lens level at 60%. Full scans were taken with the Orbitrap at 120k resolution with an automatic gain control (AGC) target of 4×10^5 charges, maximum IIT of 50 ms, and scan range of 400−1600 m/z with wide quadrupole isolation enabled. The maximum cycle time between MS^1 scans was set to 3 s.

Following the survey scan, the following filters were applied for triggering MS^2 scans. Monoisotopic peak selection was enabled and set to isolate the most abundant peak in the peptide mode. Isolated masses were excluded for 60 s after triggering

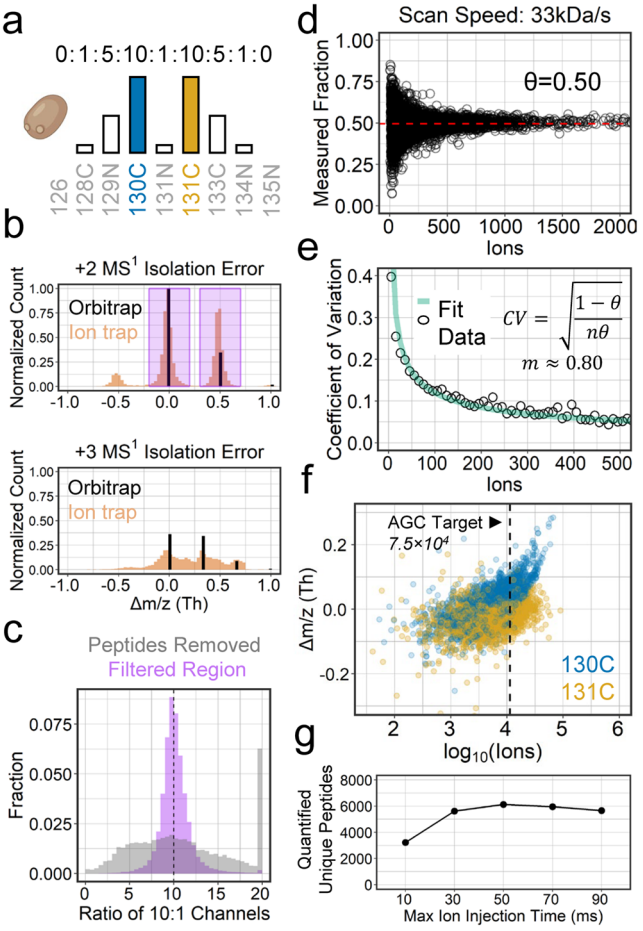

Figure 2. Optimization of the method for complement reporter ion quantification in the ion trap. (a) Yeast standard. Yeast peptides were labeled with TMTpro at defined ratios of 0:1:5:10:1:10:5:1:0 across nine channels. This standard was used for all optimization experiments shown in the figure. (b) Histogram of $\Delta m/z$ MS^1 isolation errors for 2+ and 3+ peptides. The comparatively low-resolution MS^1 scan in the ion trap leads to broader isolation errors when the isolation window is centered for the subsequent MS^2 scan. To address this, MS^2 spectra were filtered to exclude cases where isolation was not centered on the M_0 or M_{+1} precursor (i.e., peaks outside the highlighted purple region). Quantification of 3+ precursors is particularly challenging due to the narrow spacing between isotopes; therefore, all subsequent analyses were restricted to 2+ peptides. Frequency histograms are maximum-normalized and scaled by the relative charge-state contributions. (c) Precision improvement achieved by filtering based on the isolation m/z error. The purple histogram shows the distribution of peptide ratios retained after applying the isolation m/z filter (see panel b), with values tightly centered around the expected 10:1 ratio, indicating high measurement precision. In contrast, the gray histogram represents the excluded peptide data, which display a broad distribution and high quantification error. (d) Relationship between observed peptide ratios and ion counts. Using the 10:10 TMTpro channels, the measured peptide fraction was plotted against the summed ion counts. The red dashed line indicates the median measured fraction (θ), defined as TMTpro130C/(TMTpro130C + TMTpro131C). The overall data set median is 0.50, consistent with the expected 1:1 ratio. As more ions are sampled, the measured ratios converge toward this expected value, reflecting improved statistical precision. (e) Coefficients of variation (CVs) at binned ion counts were used to fit a binomial model (equation shown), yielding a conversion factor of 0.80 (m) for translating ion-trap charges into pseudocounts (n). This factor remains approximately constant across different ion-trap resolutions (Figure S2). The conversion facilitates statistical analysis and helps define signal

https://doi.org/10.1021/acs.jproteome.5c00356
J. Proteome Res. XXXX, XXX, XXX−XXX

Figure 2. continued

thresholds based on desired measurement precision. (f) Effect of ion-trap signal intensity on channel error. Channel error is plotted against $\log_{10}$-transformed ion counts for the two most abundant complement reporter ions in the yeast standard (130C and 131C). To assess the impact of signal intensity, we intentionally overfilled the ion trap using an automatic gain control (AGC) target of 1.2×10^5. When ion counts exceed ~10,000 (1×10^4), systematic m/z shifts are observed, likely due to space charging. Based on this, we selected an AGC target of 7.5×10^4 for all subsequent experiments. The dotted line indicates the expected resulting number of complement ions, a regime that minimizes measurement deviation and supports reliable quantification. (g) Ion injection time optimization. With the AGC target fixed at 7.5×10^4 and scan speed set to 33 kDa/s, we varied the ion injection time (IIT) to determine its effect on peptide quantification. An IIT of 50 ms yielded the highest number of quantified unique peptides.

with a mass tolerance window of ±10 ppm while also excluding isotopes and different charge states of the isolated species. A charge-state filter was set for 2−6+ charge states. An intensity threshold was set for 5×10^3 ions.

The following settings were used for ion-trap MS^2 scans. The AGC target was set to 1×10^4 charges, and the maximum IIT was 35 ms. The quadrupole was utilized for isolation with an isolation width of 0.7 Da, and ions were fragmented with CID at a normalized collision energy of 35% (10 ms activation time and 0.25 activation Q). The scan rate was 33 kDa/s (normal resolution) in autoscan range mode.

For triggering MS^3-scans for TMT-reporter ion-based quantification, the following filters were applied. Precursor ion exclusion was set to 5 (high) and 50 (low) m/z. Isobaric tag loss exclusion was set to TMTpro, and 10 notches were used to isolate the SPS-MS^3-precursors. MS^3 scans were acquired with a 0.7 m/z MS^1 isolation window and a 2 m/z MS^2 isolation window. The Orbitrap detector was used with a resolution of 45k and an AGC target of 2×10^5, scanning over the range 100−500 m/z. The maximum ion injection time was 86 ms. Ions were fragmented in the higher-energy collision dissociation (HCD) cell at a normalized collision energy of 45%.

TMT-MS^2 Method

TMT-MS^2 experiments were performed on the Orbitrap Lumos and Ascend. The instrument designation based on experiment is as follows: interference standard comparison with iTMTproC − Orbitrap Lumos (Figure 3), and interference standard comparison with iTMTproC − Ascend (Figure S4).

The mass spectrometer was set to analyze positively charged ions in a data-dependent MS^2 mode, recording centroid data with the RF lens level at 60%. Full scans were taken with the Orbitrap at 120k resolution with an automatic gain control (AGC) target of 4×10^5 charges, maximum IIT of 50 ms, and scan range of 350 to 1400 m/z with wide quadrupole isolation enabled. The maximum cycle time between MS^1 scans was set to 3 s.

Following the survey scan, the following filters were applied for triggering MS^2 scans. Monoisotopic peak selection was enabled and set to isolate the most abundant peak in peptide mode. Isolated masses were excluded for 60 s after triggering with a mass tolerance window of ±10 ppm while also excluding isotopes and different charge states of the isolated species. A charge-state filter was set for 2−5+ charge states.

The following settings were used for the Orbitrap MS^2 scans. The AGC target was set to 1×10^5 charges, and the maximum IIT was 96 ms. The quadrupole was utilized for isolation with an isolation width of 0.4 Da, and the ions were fragmented with HCD at a normalized collision energy of 30%. The resolution was 45,000 with a defined first mass at 110 m/z.

Data Analysis

Raw data files were analyzed using Proteome Discoverer 3.1.1.93 (Thermo Scientific) with the SEQUEST HT search engine. The database search was performed against the reference proteomes for *X. laevis* (XenBase v10.1: https://www.xenbase.org), *S. cerevisiae* (S288C: UP000002311), and *H. sapiens* (UP000005640). The search included concatenated target-decoy entries to enable the FDR estimation. For methods employing Orbitrap MS^1 scans, a precursor ion mass tolerance of 20 ppm was used, whereas iTMTproC analyses utilizing ion-trap MS^1 scans applied a tolerance of 0.7 Da. Similarly, Orbitrap MS^2 scans used a fragment ion mass tolerance of 0.02 Da, while ion-trap MS^2 scans were searched with a tolerance of 1 Da. Spectra were searched using full tryptic digestion with LysC and trypsin specificity, allowing up to two missed cleavages. *N*-Ethylmaleimide (NEM) on cysteine (+125.048 Da) and TMTpro on the peptide N-terminus and lysine were set as a static modification (+304.207 Da). Oxidation of methionine (+15.995 Da) was considered a variable modification. MS^2 spectra were selected using the Spectrum Selector node, followed by SEQUEST database searching. Percolator was used for postsearch validation, with a target-decoy strategy to control the PSM FDR at 1%. Protein-level confidence was assigned by estimating q-values derived from comparisons between target and decoy protein scores across a range of thresholds. Grouping was then performed to consolidate proteins with overlapping or nested peptide identifications, resulting in a parsimonious list of master proteins. Final protein tables were filtered to include only groups with at least one unique peptide that passed 1% protein-level FDR. For analysis of the human−yeast interference standard, only unique yeast peptides were used for quantification to avoid confounding effects from shared razor peptides between humans and yeast.

Complement ion quantification was performed using previously described methods without modification.[27,28] Briefly, the m/z of each complement reporter ion was calculated based on theoretical TMTpro fragmentation, and the observed intensities were extracted. Isotopic impurity correction was applied by using a custom R script that integrates tag-specific isotopic impurities and peptide isotopic distributions to resolve an overdetermined system via QR decomposition, yielding corrected complementary ion ratios. This pipeline was described in greater detail elsewhere,[27,28] and the quantification module is scheduled for inclusion in an upcoming release of Proteome Discoverer. For iTMTproC, PSMs were filtered based on the following criteria: charge = 2, theoretical m/z <1075, and M_0/M_1 isolation error $\Delta m/z$ ±0.2. Complement ion intensities from redundant PSMs passing all filters were summed to retain a usable signal that would otherwise be discarded. An intensity threshold of 563 ions was used, corresponding to an expected CV of 10% as described above.[41]

For reporter ion quantification, reporter ion intensities were extracted in the Reporter Ion Quantifier node of the Proteome Discoverer. For non-RTS MultiNotch MS^3 workflows, only PSMs with coisolation interference below 25%, SPS matches above 45%, and signal-to-noise ratios of at least 129 for 2+ peptides and 265 for 3+ peptides were retained for quantification. This signal threshold matches the ion statistical

https://doi.org/10.1021/acs.jproteome.5c00356
J. Proteome Res. XXXX, XXX, XXX−XXX

criteria of iTMTproC with an expected CV of 10%.[27,41] Protein-level quantification was performed using the median reporter ion intensity across all PSMs assigned to each protein group. TMT-MS^2 used the same quantification workflow but excluded the SPS match requirement when filtering PSMs.

RESULTS AND DISCUSSION

Optimizing Complement Reporter Ion Quantification in Ion Traps

To establish robust parameters for iTMTproC on quadrupole−ion trap instruments, we adapted previously described TMTproC methods, originally developed for quadrupole−Orbitrap analyzers.[27] Adjustments were necessary to accommodate the lower-resolution characteristic of the ion-trap MS^1 and MS^2 scans. Additionally, we refined dynamic exclusion settings based on parameters optimized for label-free ion-trap experiments.[42] This included addressing a marked discrepancy in peptide-spectrum match (PSM) yields between the simple linear discriminant analysis (LDA) classifier or the more sophisticated Percolator.[43,44] Interestingly, Percolator identifies substantially more PSMs from MS^1 ion-trap data (Figure S1), while there is little difference between the classifiers when using MS^1 Orbitrap data. We therefore used a Percolator for all subsequent analyses. We evaluated peptide identification and quantification performance using a defined yeast peptide standard labeled with TMTpro at ratios of 0:1:5:10:1:10:5:1:0 across the nine complementary ion channels (Figure 2a). A significant challenge for implementing TMTproC in ion traps was the comparatively low-mass accuracy during the MS^1 scans. This limited accuracy complicates quadrupole isolation, particularly in distinguishing closely spaced isotopic peaks (e.g., M_0 and M_{+1}). Consequently, multiple peaks can be inadvertently coisolated, undermining accurate selection of the intended peak, which is critical for reliable quantification in TMTproC workflows (Figure 2b). To address this challenge, we introduced a filtering step targeting doubly charged (2+) peptides. Specifically, we limited the quadrupole isolation window to ±0.2 Th around the theoretical M_0 and M_{+1} peptide m/z values, significantly improving the quantification accuracy (Figure 2c). In principle, triply charged (3+) precursor peptides could also be quantified, though this would require an even narrower quadrupole isolation window around theoretical M_0 and M_{+1} peaks. However, minor calibration drifts of the quadrupole introduced noticeable quantification distortion for these peptides. To ensure robustness and reproducibility, we excluded 3+ precursor peptides from subsequent analyses in this study. This filtering step resulted in a 19% reduction in unique quantifiable peptides (from 7359 to 5995 peptides). Despite this decrease, we demonstrate subsequently that the overall number of quantified peptides and proteins remain highly competitive, confirming the effectiveness and practicality of this optimized approach.

Next, we established the relationship between raw ion signals (denormalized by the ion injection time) and pseudocounts derived from a binomial statistical model. In this framework, each detected complement reporter ion is treated as an independent sampling event, with a fixed probability of being assigned to a given channel. For a 1:1 ratio comparison, each ion has a 50% chance of being detected in either channel. The variability in the measured ratios is determined by the number of ions sampled. Because the process involves a finite number of discrete independent assignments to one of the two possible outcomes, the binomial model appropriately captures the statistical behavior.[41] Defining this relationship is essential for setting appropriate signal thresholds corresponding to the desired measurement precision. To determine the conversion factor between ions and pseudocounts, we analyzed peptide ratios from the equally mixed 10:10 TMTpro channels in our yeast standard, plotting these ratios against their summed ion counts (Figure 2a,d). With fewer ions sampled, the measured ratios showed high variability due to statistical fluctuations. As the ion sampling increased, these ratios converged toward the expected 1:1 ratio, consistent with predictions from the binomial model. From the relationship between the expected coefficient of variation (CV) and pseudocounts, we derived a conversion factor of approximately 0.8 pseudocounts per ion. We confirmed the consistency of this conversion factor across various ion-trap scan speeds ranging from 66 to 2 kDa/s (rapid, normal, enhanced, and zoom; Figure S2). This finding contrasts with Orbitrap-based methods, where higher analyzer resolution typically results in smaller conversion factors.[41,45,46] Based on this analysis, we established a minimum pseudocount threshold of 450 in the nine resolvable TMTproC channels, corresponding to an expected coefficient of variation (CV) of ∼10% for a 1:1 ratio across all channels.

We then optimized two additional critical parameters: the automatic gain control (AGC) and ion injection time (IIT), specifically for iTMTproC. Like Orbitrap analyzers, ion traps are susceptible to space charging, where the accumulation of too many ions leads to mutual repulsion that distorts the measured m/z values.[45,47] However, the ion-trap spectral space-charge limit is much lower than that of the Orbitrap, making accurate control of ion load especially important. To empirically determine the ion trap's upper capacity limit, we deliberately overloaded the ion trap using a high AGC target of 1.2×10^5. We then evaluated the mass accuracy of complement reporter ions as a function of the total ion intensity in their respective channels (Figure 2f). This experiment used the yeast-only standard shown in Figure 2a and focused on channels 130C and 131C, which represent the two most abundant channels in that sample and are therefore expected to show the earliest signs of space-charge-induced distortion. As the total ion counts increased, both channels exhibited a clear upward shift in m/z error, consistent with the onset of space-charge-induced distortion. This shift became noticeable above 10^4, which approximately corresponds to an AGC target of 7.5×10^4 when accounting for the ∼15% efficiency of complement ion generation.[27] Based on this analysis, we selected 7.5×10^4 as the AGC target for all subsequent analyses, as it maximized ion sampling while minimizing space-charge-related shifts in mass accuracy.

Lastly, we optimized the ion injection time by varying IIT values systematically from 10 to 90 ms (Figure 2g). We assessed each IIT setting based on the number of uniquely quantified peptides meeting our previously established quality criteria (pseudocount >450 and ±0.2 Th isolation window filter). An IIT of 50 ms yielded the highest number of quantified peptides. Taken together, these experiments established the final AGC (7.5×10^4) and IIT (50 ms) parameters for iTMTproC, enabling robust and accurate quantification on quadrupole−ion trap instrumentation. Detailed experimental procedures outlining these optimized settings are provided in the Experimental Procedures section, and those settings were applied throughout the remainder of this study.

https://doi.org/10.1021/acs.jproteome.5c00356
J. Proteome Res. XXXX, XXX, XXX−XXX

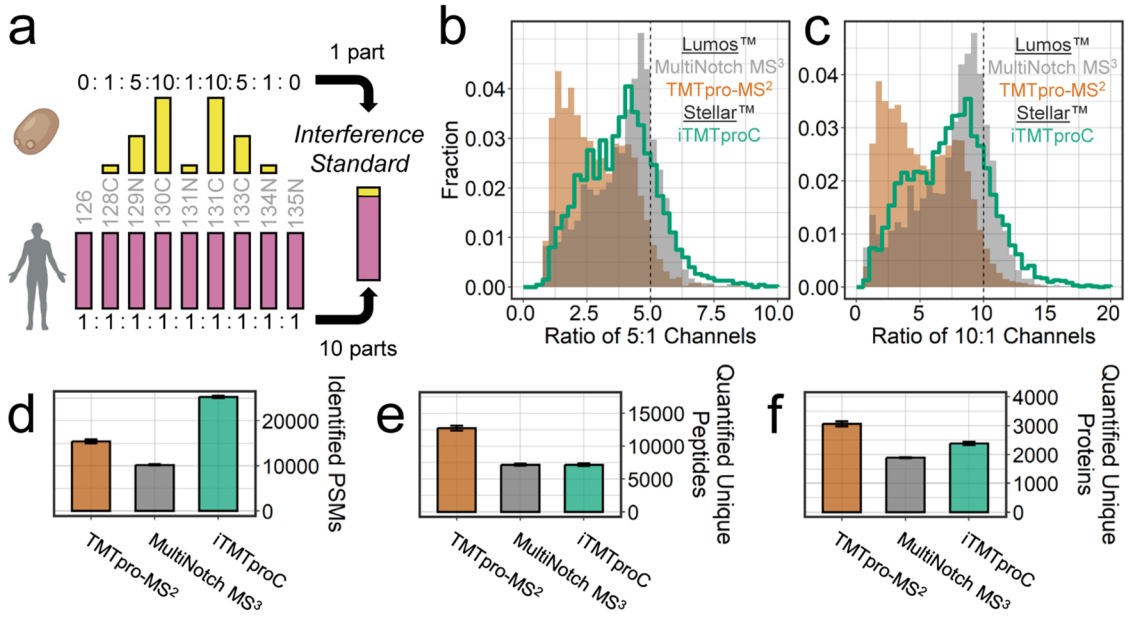

Figure 3. Multiplexed iTMTproC shotgun proteomics on Stellar yields results comparable to MultiNotch MS^3 on the Orbitrap Lumos. (a) Human−yeast interference standard. Yeast peptides were labeled with TMTpro in defined ratios of 0:1:5:10:1:10:5:1:0 and combined with HeLa peptides labeled 1:1:1:1:1:1:1:1:1:1 across the same channels. To simulate the interference encountered with dynamic, typically low-abundance proteins, the samples were mixed in a 1:10 yeast-to-human ratio. (b, c) Ratio distortion comparison of iTMTproC on Stellar vs MultiNotch MS^3 on the Orbitrap Lumos. Histograms of measured ratios for the 5:1 (b) and 10:1 (c) yeast channels. Ratios closer to the expected values indicate reduced interference and improved quantification accuracy. While MultiNotch MS^3 on the Orbitrap Lumos shows slightly higher accuracy, both methods substantially outperform TMTpro-MS^2-based quantification on the Orbitrap Lumos. (d) Number of peptide-spectrum matches (PSMs). iTMTproC yields the highest number of PSMs, driven by its fast scan speed, high sensitivity of the ion trap, and repeated targeting of the same isotopic envelope. Error bars represent the standard error of the mean (n = 3). (e) Number of quantified unique peptides. TMTpro-MS^2 yields the highest number of unique quantified peptides; however, these measurements are often severely distorted due to interference. The number of unique quantified peptides is nearly identical between those of Stellar iTMTproC and Orbitrap Lumos MultiNotch MS^3. Although iTMTproC shows a lower conversion rate from PSMs to unique peptides—due to stringent filtering and redundancy—this is compensated by its higher total PSM count, resulting in comparable peptide-level coverage. (f) Number of quantified proteins. TMTpro-MS^2 on the Orbitrap quantifies the highest number of proteins, though these measurements suffer from severe ratio distortion. On average, Stellar iTMTproC quantifies 26% more proteins than Orbitrap Lumos MultiNotch MS^3 in a single-shot analysis.

Evaluating Stellar iTMTproc with an Interference Standard against Orbitrap Lumos MultiNotch MS^3

Next, we evaluated iTMTproC with a standard that combines two samples (yeast and human) with differing mixing ratios[19,20] (Figure 3a). We combined one part yeast versus ten parts human to simulate interference for biologically dynamic proteins, which tend to be of low abundance.[26,48] We have chosen to compare those results with MultiNotch MS^3 on the Orbitrap Lumos due to its proven track record in generating highly valuable data that have led to numerous biological insights.[49−54] First, we varied ion-trap scan speeds from 66 kDa/s (rapid) to 2 kDa/s (zoom) and determined how this would affect the observed interference (Figure S3). Higher resolution helps distinguish the real signal from background noise. However, the higher resolution in the ion trap comes at the cost of dramatically slower scan speeds (Figure S3e). Based on our previous finding that our desired IIT is 50 ms, we chose 33 kDa/s (normal) for iTMTproC analysis, which takes approximately 36 ms to scan an MS^2 spectrum with a 1200 m/z range (Figure S3e). Importantly, the ion injection time and ion-trap m/z analysis are parallelized on the quadrupole−ion trap instruments, and the 33 kDa/s scanning resolution therefore does not significantly slow down iTMTproC analysis.

Next, we assessed quantification accuracy by examining measured ratio distributions for yeast peptides in the 5:1 and 10:1 channels, which served as indicators of interference levels (Figure 3b,c). While MultiNotch MS^3 on the Orbitrap Lumos exhibited slightly less ratio distortion, Stellar iTMTproC minimized interference, producing distributions that closely aligned with the MS^3 data. Significantly, both methods represented a substantial improvement over TMTpro-MS^2 reporter ion quantification in the Orbitrap, where low-m/z reporter ions are more susceptible to coisolation interference.

We also evaluated method sensitivity and found that iTMTproC on Stellar quantified about the same number of unique peptides as Orbitrap Lumos MS^3 while quantifying 30% more proteins (Figure 3d−f). This was likely due to iTMTproC's capability to quantify lower abundant 2+ peptides, while MultiNotch MS^3 quantified 3+ peptides, which added new unique peptides but tended to come from the highest abundant proteins that were already quantified. It is important to note that this difference in protein identifications is most pronounced in single-shot analyses; in applications where prefractionation is used to distribute peptides across multiple fractions, the difference becomes less pronounced but still noticeable, as shown in a later section.

Comparing methods between different instruments, associated HPLCs, and laboratories has the inherent caveat that it is unclear how much of the observed differences are due to the actual methods versus instrument or HPLC calibration, instrument performance, and setups. To minimize this possibility for biases, we evaluated iTMTproC, TMTpro-MS^2,

https://doi.org/10.1021/acs.jproteome.5c00356
J. Proteome Res. XXXX, XXX, XXX−XXX

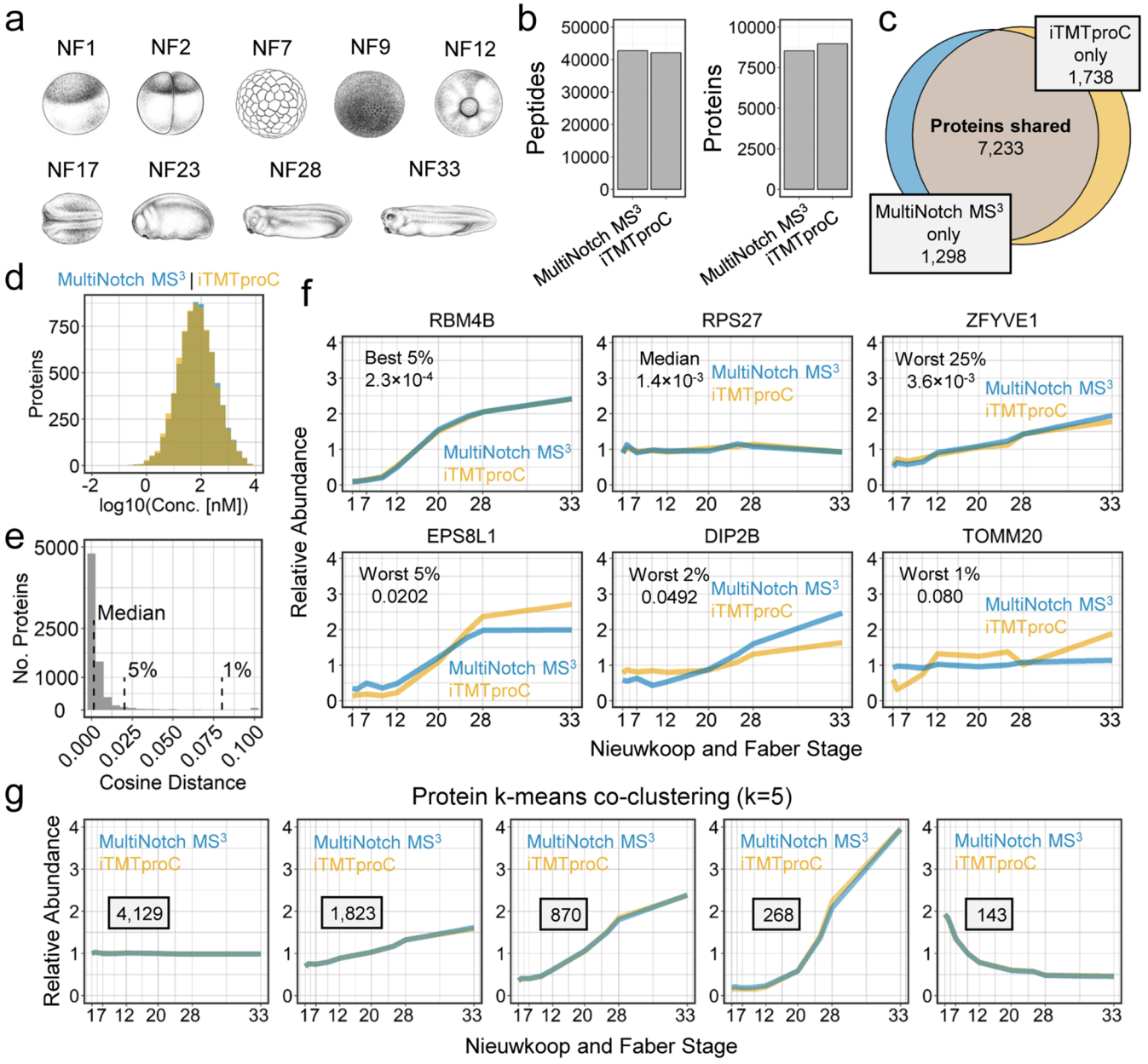

Figure 4. Comparing iTMTproC with MultiNotch MS^3 to analyze proteomic changes across developing frog embryos. (a) Developmental stages of the frog *Xenopus laevis*. Embryos were collected at defined Nieuwkoop and Faber stages[37] and labeled with TMTpro reagents for quantitative proteomic analysis using both iTMTproC and MultiNotch MS^3. *Xenopus* illustrations from Zahn.[39] (b) Quantified unique peptides and proteins from 24 fractions. MultiNotch MS^3 quantified slightly more unique peptides, while iTMTproC quantified approximately 5% more proteins. (c) Venn diagram of quantified proteins. Most proteins are quantified by both methods with a slightly larger number uniquely quantified by iTMTproC. (d) Distribution of the absolute protein concentrations. Both iTMTproC and MultiNotch MS^3 capture a similar dynamic range of protein abundances.[40] (e) Cosine distance histogram between iTMTproC and MultiNotch MS^3 measurements. Histogram of cosine distances for proteins quantified by both methods. Vertical lines indicate the median (distance = 1.4×10^{-3}), 95th, and 99th percentiles. The distribution shows that most proteins exhibit highly similar expression profiles independent of the quantification method. (f) Representative examples of protein quantification. Shown are proteins at the fifth percentile (RBM4B), median (RPS27), 75th percentile (ZFYVE1), 95th percentile (EPS8L1), 98th percentile (DIP2B), and 99th percentile (TOMM20) based on the cosine distance between the two methods. Even proteins in the most distant 2% exhibit similar expression trends. Only the most divergent 1% shows substantial disagreement. The *x*-axis is scaled by hours postfertilization. (g) Protein *k*-means coclustering ($k = 5$). Coclustering of proteins across paired developmental time points reveals nearly identical expression dynamics between iTMTproC and MultiNotch MS^3, highlighting the high concordance and comparable data quality between the two methods.

and MultiNotch MS^3 (non-RTS) on a single HPLC (Vanquish Neo) and a single mass spectrometer (Ascend) (Figure S4). The Ascend quadrupole and low-pressure ion trap used for m/z analysis are identical to the standalone quadrupole−ion trap (Stellar), though the Ascend incorporates a larger high-pressure trap to support a higher space-charge capacity for techniques such as electron-transfer dissociation. Compared to the Orbitrap Lumos, the Ascend quadrupole is a significant advancement with higher ion-transfer efficiency and a more ideal, rectangular transmission profile.[55] The increased selectivity and sensitivity are expected to result in data from MS^3 and TMT-MS^2 that would outperform data acquired with these methods on the

https://doi.org/10.1021/acs.jproteome.5c00356
J. Proteome Res. XXXX, XXX, XXX−XXX

Orbitrap Lumos. Nevertheless, comparing iTMTproC, MultiNotch MS^3, and TMTpro-MS^2 on a single instrument mirrored the results of comparison between Stellar and Orbitrap Lumos—iTMTproC exhibited higher sensitivity than MultiNotch MS^3 but slightly lower accuracy while still providing substantially improved data quality over TMTpro-MS^2 (Figure S4). Overall, we conclude that iTMTproC is able to obtain accurate multiplexed proteomic data with slightly more ratio distortion than MultiNotch MS^3. However, this is compensated for by a slightly larger number of quantified proteins.

Evaluating iTMTproC and MultiNotch MS^3 in a Complex Biological Sample

To evaluate the practical applicability of iTMTproC beyond controlled standards, we tested its performance using complex biological samples. Specifically, we assessed protein dynamics during early embryonic development of the frog *Xenopus laevis*, tracking changes from fertilized eggs to swimming tadpoles (Figure 4). At each developmental time point, we collected four embryos, prepared protein samples following established protocols, and performed prefractionation via medium-pH reverse-phase chromatography.[32,35] We then analyzed 24 fractions using both iTMTproC and MultiNotch MS^3 on an Ascend instrument. Both methods quantified similar numbers of unique peptides; however, iTMTproC identified 8,971 proteins compared to 8,531 proteins quantified by MultiNotch MS^3—approximately a 5% increase in proteome coverage—highlighting iTMTproC's enhanced sensitivity (Figure 4b). The proteins identified by both methods showed substantial overlap (Figure 4c). To further evaluate proteome coverage, we compared quantified proteins against a reference data set of absolute protein abundances measured previously in *Xenopus laevis* eggs.[40] Protein abundance distributions were nearly identical across methods (Figure 4d), confirming a similar dynamic range coverage. Notably, the total number of proteins quantified by either approach surpassed previously published results from our lab using a similar developmental time-series analyzed with MultiNotch MS^3 (TMT10plex) on an Orbitrap Lumos, which quantified 7827 proteins after reanalysis with updated gene models.[31] These findings demonstrate that iTMTproC delivers data quality and proteome coverage comparable to what was achievable with state-of-the-art multiplexed shotgun proteomic methods just a few years ago.

While the number of quantified proteins is promising, even more critical is the agreement between protein dynamics measured by different quantification methods. To assess this quantitatively, we calculated cosine distances across the nine developmental time points for all proteins quantified by both iTMTproC and MultiNotch MS^3 (Figure 4e). The resulting distribution of cosine distances showed a median value of 1.4×10^{-3}, indicating high overall similarity between temporal protein profiles obtained from the two approaches. However, biological interpretation of cosine distances can be challenging. To illustrate the biological meaning of these metrics more intuitively, we selected proteins representing the 5th, 50th, 75th, 95th, and 99th percentiles of agreement (with lower percentiles reflecting a closer agreement) and plotted their developmental dynamics (Figure 4f). Encouragingly, protein dynamics remained essentially indistinguishable up to the 75th percentile of proteins. Even proteins at the 95th percentile (EPS8L1) and 98th percentile (DIP2B) exhibited similar overall dynamic trends. Only at the extreme (99th percentile, TOMM20) did substantial disagreement between the two methods become apparent. Given that both data sets were stringently controlled at a 1% false discovery rate (FDR) at both the peptide and protein levels, such discrepancies at the extreme percentile are expected.

The consistency of these measurements between iTMTproC and MultiNotch MS^3 was further supported by global trends in protein expression. *k*-means clustering (k = 5) of protein dynamics revealed highly similar developmental expression profiles across all clusters between the two methods (Figure 4g). Collectively, these analyses emphasize that in practical biological applications the system-level data generated by iTMTproC on quadrupole−ion trap instrumentation and MultiNotch MS^3 are essentially equivalent.

CONCLUSIONS

In this study, we demonstrated that complement reporter ion quantification can be successfully adapted to quadrupole−ion trap instrumentation for multiplexed shotgun proteomics (iTMTproC). Benchmarking with defined standards and complex biological samples reveals that iTMTproC achieves quantification accuracy and interference reduction comparable to those of established MultiNotch MS^3 methods on high-end Orbitrap instruments. Although iTMTproC currently exhibits higher ratio compression and lower sensitivity compared to the latest specialized multiplexing approaches,[24,28] it importantly enables multiplexed quantitative analysis on cost-effective quadrupole−ion trap platforms. This advance significantly expands accessibility and helps democratize advanced quantitative proteomics. Additionally, while our study focuses on nanoflow LC separations, the robust performance of iTMTproC also raises the possibility of adapting this method to alternative separation strategies, such as capillary electrophoresis (CE).[56] Until now, quadrupole−ion trap instruments such as Stellar have primarily been employed for targeted analyses. In this context, iTMTproC represents an attractive option for increasing sample multiplexing without compromising assay throughput, as often encountered with slower MS^3-based methods.[57] Our findings also highlight previously underappreciated multiplexing capabilities of ion-trap analyzers, which traditionally have been confined to qualitative or targeted proteomic applications.[11,58] In future work, it will be particularly interesting to investigate whether the multiplexing strategy demonstrated here can be effectively applied to multiplexed targeted proteomic workflows.

While iTMTproC on the Stellar demonstrates quantification performance comparable to that of MultiNotch MS^3 workflows on Orbitrap-based systems, it is important to contextualize these results within the broader landscape of advanced multiplexed proteomic technologies. The iTMTproC implementation is limited to nine channels, whereas Orbitrap-based TMT workflows now support up to 35-plex analyses, though only 18 channels can be used without deuterium-induced elution shifts.[30] For specialized laboratories prioritizing maximum throughput and data quality, high-end tribrid instruments like the Orbitrap Ascend are likely the preferred solution. However, iTMTproC meaningfully extends multiplexed shotgun proteomic capabilities to instruments already optimized for targeted workflows. We aim for these added "free" capabilities to be useful to such laboratories and also help lower the barrier to entry, enabling new laboratories to adopt affordable instrumentation capable of both targeted and discovery proteomics.

In this study, we implemented iTMTproC by isolating ions by using the quadrupole. However, ion traps themselves can, in principle, also achieve effective ion isolation. In configurations

https://doi.org/10.1021/acs.jproteome.5c00356
J. Proteome Res. XXXX, XXX, XXX−XXX

with adjacent higher-energy collision dissociation (HCD) cells, where ions are injected simultaneously into the trap, space-charging effects can become particularly challenging—especially for the narrow isolation windows required by iTMTproC—reducing isolation effectiveness and quantification accuracy. Nevertheless, this limitation could potentially be overcome in instruments designed for the continuous ion transfer into the trap. In future work, we plan to evaluate whether robust iTMTproC quantification can be achieved on ion-trap-only instruments. Demonstrating this capability would further reduce instrument costs and has the potential to significantly expand access for quantitative proteomics in nonspecialized laboratories.

■ ASSOCIATED CONTENT

Data Availability Statement

The MS proteomic data generated in this study have been deposited to the ProteomeXChange Consortium via the PRIDE[59] partner repository with the data set identifier PXD062540.

Supporting Information

The Supporting Information is available free of charge at https://pubs.acs.org/doi/10.1021/acs.jproteome.5c00356.

> Comparison of the postsearch classification strategy on peptide identification in MS^1 ion trap vs Orbitrap data; scan speed does not affect the conversion factor between charges and pseudocounts in an ion trap; evaluation of ion-trap scan speeds for iTMTproC quantification using the human−yeast interference standard; and comparison of iTMTproC with MultiNotch MS^3 and TMTpro-MS^2 on the Ascend. (PDF)

■ AUTHOR INFORMATION

Corresponding Authors

Philip M. Remes − *Thermo Fisher Scientific, San Jose, California 95134, United States*; Email: philip.remes@thermofisher.com

Martin Wühr − *Department of Molecular Biology, Princeton University, Princeton, New Jersey 08544, United States; Lewis-Sigler Institute for Integrative Genomics and Department of Chemical and Biological Engineering, Princeton University, Princeton, New Jersey 08544, United States*; Email: wuhr@princeton.edu

Authors

Edward R. Cruz − *Department of Molecular Biology, Princeton University, Princeton, New Jersey 08544, United States; Lewis-Sigler Institute for Integrative Genomics, Princeton University, Princeton, New Jersey 08544, United States*; orcid.org/0000-0001-6454-1461

Alex N. T. Johnson − *Department of Molecular Biology, Princeton University, Princeton, New Jersey 08544, United States; Lewis-Sigler Institute for Integrative Genomics and Department of Chemical and Biological Engineering, Princeton University, Princeton, New Jersey 08544, United States*

Vyas Pujari − *Department of Molecular Biology, Princeton University, Princeton, New Jersey 08544, United States; Lewis-Sigler Institute for Integrative Genomics, Princeton University, Princeton, New Jersey 08544, United States*

Qi Zhang − *Lewis-Sigler Institute for Integrative Genomics and Department of Chemical and Biological Engineering, Princeton University, Princeton, New Jersey 08544, United States*

Thao Nguyen − *Department of Molecular Biology, Princeton University, Princeton, New Jersey 08544, United States; Lewis-Sigler Institute for Integrative Genomics and Department of Chemical and Biological Engineering, Princeton University, Princeton, New Jersey 08544, United States*

Michael Stadlmeier − *Department of Molecular Biology, Princeton University, Princeton, New Jersey 08544, United States; Lewis-Sigler Institute for Integrative Genomics, Princeton University, Princeton, New Jersey 08544, United States*

Jessica Wang − *Lewis-Sigler Institute for Integrative Genomics, Princeton University, Princeton, New Jersey 08544, United States*

Cristina C. Jacob − *Thermo Fisher Scientific, San Jose, California 95134, United States*

Graeme C. McAlister − *Thermo Fisher Scientific, San Jose, California 95134, United States*

Complete contact information is available at: https://pubs.acs.org/10.1021/acs.jproteome.5c00356

Notes

The authors declare the following competing financial interest(s): GCM, PMR, and CJ are employees of Thermo Fisher Scientific. Thermo Fisher provides limited support to MW laboratory under a collaborative research agreement with Princeton University. All other authors declare they have no conflicts of interest with the contents of this article.

■ ACKNOWLEDGMENTS

This work was supported by the National Institutes of Health grant R35GM128813 (M.W.). We gratefully acknowledge support from the Princeton Catalysis Initiative and the Eric and Wendy Schmidt Transformative Technology Fund. We are grateful to Dean Edelman and his colleagues in the Office of the Dean of Research for their support in enabling this study. We gratefully acknowledge support from the American Heart Association predoctoral fellowship 20PRE35220061 (T.N.) and the NSF Graduate Research Fellowship (E.R.C.). We thank Matthew The and Mark Schroeder for their help in setting up the peptide classifier. We thank Eric Wieschaus and Trudi Schüpbach for useful discussions and suggestions during the writing of this manuscript. The content of this article is solely the responsibility of the authors and does not necessarily represent the official views of the National Institutes of Health.

■ REFERENCES

(1) Addona, T. A.; Abbatiello, S. E.; Schilling, B.; Skates, S. J.; Mani, D. R.; Bunk, D. M.; Spiegelman, C. H.; Zimmerman, L. J.; Ham, A. J.; Keshishian, H.; et al. Multi-site assessment of the precision and reproducibility of multiple reaction monitoring-based measurements of proteins in plasma. *Nat. Biotechnol.* **2009**, *27* (7), 633−641.

(2) Manes, N. P.; Nita-Lazar, A. Application of targeted mass spectrometry in bottom-up proteomics for systems biology research. *J. Proteomics* **2018**, *189*, 75−90.

(3) Pappireddi, N.; Martin, L.; Wuhr, M. A Review on Quantitative Multiplexed Proteomics. *ChemBioChem* **2019**, *20* (10), 1210−1224.

(4) Anderson, L.; Hunter, C. L. Quantitative mass spectrometric multiple reaction monitoring assays for major plasma proteins. *Mol. Cell Proteomics* **2006**, *5* (4), 573−588.

(5) Kelstrup, C. D.; Young, C.; Lavallee, R.; Nielsen, M. L.; Olsen, J. V. Optimized fast and sensitive acquisition methods for shotgun proteomics on a quadrupole orbitrap mass spectrometer. *J. Proteome Res.* **2012**, *11* (6), 3487−3497.
(6) Wilhelm, M.; Schlegl, J.; Hahne, H.; Gholami, A. M.; Lieberenz, M.; Savitski, M. M.; Ziegler, E.; Butzmann, L.; Gessulat, S.; Marx, H.; et al. Mass-spectrometry-based draft of the human proteome. *Nature* **2014**, *509* (7502), 582−587.
(7) Gerber, S. A.; Rush, J.; Stemman, O.; Kirschner, M. W.; Gygi, S. P. Absolute quantification of proteins and phosphoproteins from cell lysates by tandem MS. *Proc. Natl. Acad. Sci. U.S.A.* **2003**, *100* (12), 6940−6945.
(8) Picotti, P.; Bodenmiller, B.; Mueller, L. N.; Domon, B.; Aebersold, R. Full dynamic range proteome analysis of S. cerevisiae by targeted proteomics. *Cell* **2009**, *138* (4), 795−806.
(9) Kuzyk, M. A.; Smith, D.; Yang, J.; Cross, T. J.; Jackson, A. M.; Hardie, D. B.; Anderson, N. L.; Borchers, C. H. Multiple reaction monitoring-based, multiplexed, absolute quantitation of 45 proteins in human plasma. *Mol. Cell Proteomics* **2009**, *8* (8), 1860−1877.
(10) Bereman, M. S.; MacLean, B.; Tomazela, D. M.; Liebler, D. C.; MacCoss, M. J. The development of selected reaction monitoring methods for targeted proteomics via empirical refinement. *Proteomics* **2012**, *12* (8), 1134−1141.
(11) Remes, P. M.; Jacob, C. C.; Heil, L. R.; Shulman, N.; MacLean, B. X.; MacCoss, M. J. Hybrid Quadrupole Mass Filter-Radial Ejection Linear Ion Trap and Intelligent Data Acquisition Enable Highly Multiplex Targeted Proteomics. *J. Proteome Res.* **2024**, *23* (12), 5476−5486.
(12) Xiang, F.; Ye, H.; Chen, R.; Fu, Q.; Li, L. N,N-dimethyl leucines as novel isobaric tandem mass tags for quantitative proteomics and peptidomics. *Anal. Chem.* **2010**, *82* (7), 2817−2825.
(13) Gillet, L. C.; Navarro, P.; Tate, S.; Rost, H.; Selevsek, N.; Reiter, L.; Bonner, R.; Aebersold, R. Targeted data extraction of the MS/MS spectra generated by data-independent acquisition: a new concept for consistent and accurate proteome analysis. *Mol. Cell Proteomics* **2012**, *11* (6), No. e016717.
(14) Meier, F.; Brunner, A. D.; Frank, M.; Ha, A.; Bludau, I.; Voytik, E.; Kaspar-Schoenefeld, S.; Lubeck, M.; Raether, O.; Bache, N.; et al. diaPASEF: parallel accumulation-serial fragmentation combined with data-independent acquisition. *Nat. Methods* **2020**, *17* (12), 1229−1236.
(15) Salovska, B.; Li, W.; Di, Y.; Liu, Y. BoxCarmax: A High-Selectivity Data-Independent Acquisition Mass Spectrometry Method for the Analysis of Protein Turnover and Complex Samples. *Anal. Chem.* **2021**, *93* (6), 3103−3111.
(16) Liu, X.; Dawson, S. L.; Gygi, S. P.; Paulo, J. A. Isobaric Tagging and Data Independent Acquisition as Complementary Strategies for Proteome Profiling on an Orbitrap Astral Mass Spectrometer. *J. Proteome Res.* **2025**, *24* (3), 1414−1424.
(17) Thompson, A.; Schafer, J.; Kuhn, K.; Kienle, S.; Schwarz, J.; Schmidt, G.; Neumann, T.; Johnstone, R.; Mohammed, A. K.; Hamon, C. Tandem mass tags: a novel quantification strategy for comparative analysis of complex protein mixtures by MS/MS. *Anal. Chem.* **2003**, *75* (8), 1895−1904.
(18) Li, J.; Cai, Z.; Bomgarden, R. D.; Pike, I.; Kuhn, K.; Rogers, J. C.; Roberts, T. M.; Gygi, S. P.; Paulo, J. A. TMTpro-18plex: The Expanded and Complete Set of TMTpro Reagents for Sample Multiplexing. *J. Proteome Res.* **2021**, *20* (5), 2964−2972.
(19) Ting, L.; Rad, R.; Gygi, S. P.; Haas, W. MS3 eliminates ratio distortion in isobaric multiplexed quantitative proteomics. *Nat. Methods* **2011**, *8* (11), 937−940.
(20) Wenger, C. D.; Lee, M. V.; Hebert, A. S.; McAlister, G. C.; Phanstiel, D. H.; Westphall, M. S.; Coon, J. J. Gas-phase purification enables accurate, multiplexed proteome quantification with isobaric tagging. *Nat. Methods* **2011**, *8* (11), 933−935.
(21) Schweppe, D. K.; Prasad, S.; Belford, M. W.; Navarrete-Perea, J.; Bailey, D. J.; Huguet, R.; Jedrychowski, M. P.; Rad, R.; McAlister, G.; Abbatiello, S. E.; et al. Characterization and Optimization of Multiplexed Quantitative Analyses Using High-Field Asymmetric-Waveform Ion Mobility Mass Spectrometry. *Anal. Chem.* **2019**, *91* (6), 4010−4016.
(22) McAlister, G. C.; Nusinow, D. P.; Jedrychowski, M. P.; Wuhr, M.; Huttlin, E. L.; Erickson, B. K.; Rad, R.; Haas, W.; Gygi, S. P. MultiNotch MS3 enables accurate, sensitive, and multiplexed detection of differential expression across cancer cell line proteomes. *Anal. Chem.* **2014**, *86* (14), 7150−7158.
(23) Erickson, B. K.; Mintseris, J.; Schweppe, D. K.; Navarrete-Perea, J.; Erickson, A. R.; Nusinow, D. P.; Paulo, J. A.; Gygi, S. P. Active Instrument Engagement Combined with a Real-Time Database Search for Improved Performance of Sample Multiplexing Workflows. *J. Proteome Res.* **2019**, *18* (3), 1299−1306.
(24) Schweppe, D. K.; Eng, J. K.; Yu, Q.; Bailey, D.; Rad, R.; Navarrete-Perea, J.; Huttlin, E. L.; Erickson, B. K.; Paulo, J. A.; Gygi, S. P. Full-Featured, Real-Time Database Searching Platform Enables Fast and Accurate Multiplexed Quantitative Proteomics. *J. Proteome Res.* **2020**, *19* (5), 2026−2034.
(25) Wühr, M.; Haas, W.; McAlister, G. C.; Peshkin, L.; Rad, R.; Kirschner, M. W.; Gygi, S. P. Accurate multiplexed proteomics at the MS2 level using the complement reporter ion cluster. *Anal. Chem.* **2012**, *84* (21), 9214−9221.
(26) Sonnett, M.; Yeung, E.; Wuhr, M. Accurate, Sensitive, and Precise Multiplexed Proteomics Using the Complement Reporter Ion Cluster. *Anal. Chem.* **2018**, *90* (8), 5032−5039.
(27) Johnson, A.; Stadlmeier, M.; Wuhr, M. TMTpro Complementary Ion Quantification Increases Plexing and Sensitivity for Accurate Multiplexed Proteomics at the MS2 Level. *J. Proteome Res.* **2021**, *20* (6), 3043−3052.
(28) Johnson, A. N. T.; Huang, J.; Marishta, A.; Cruz, E. R.; Mariossi, A.; Barshop, W. D.; Canterbury, J. D.; Melani, R.; Bergen, D.; Zabrouskov, V.; et al. Sensitive and Accurate Proteome Profiling of Embryogenesis Using Real-Time Search and TMTproC Quantification. *Mol. Cell Proteomics* **2025**, *24* (2), No. 100899.
(29) Kozhinov, A. N.; Johnson, A.; Nagornov, K. O.; Stadlmeier, M.; Martin, W. L.; Dayon, L.; Corthesy, J.; Wuhr, M.; Tsybin, Y. O. Super-Resolution Mass Spectrometry Enables Rapid, Accurate, and Highly Multiplexed Proteomics at the MS2 Level. *Anal. Chem.* **2023**, *95* (7), 3712−3719.
(30) Zuniga, N. R.; Frost, D. C.; Kuhn, K.; Shin, M.; Whitehouse, R. L.; Wei, T. Y.; He, Y.; Dawson, S. L.; Pike, I.; Bomgarden, R. D.; et al. Achieving a 35-Plex Tandem Mass Tag Reagent Set through Deuterium Incorporation. *J. Proteome Res.* **2024**, *23* (11), 5153−5165.
(31) Gupta, M.; Sonnett, M.; Ryazanova, L.; Presler, M.; Wuhr, M. Quantitative Proteomics of Xenopus Embryos I, Sample Preparation. *Methods Mol. Biol.* **2018**, *1865*, 175−194.
(32) Wühr, M.; Guttler, T.; Peshkin, L.; McAlister, G. C.; Sonnett, M.; Ishihara, K.; Groen, A. C.; Presler, M.; Erickson, B. K.; Mitchison, T. J.; et al. The Nuclear Proteome of a Vertebrate. *Curr. Biol.* **2015**, *25* (20), 2663−2671.
(33) Wessel, D.; Flugge, U. I. A method for the quantitative recovery of protein in dilute solution in the presence of detergents and lipids. *Anal. Biochem.* **1984**, *138* (1), 141−143.
(34) Hughes, C. S.; Moggridge, S.; Muller, T.; Sorensen, P. H.; Morin, G. B.; Krijgsveld, J. Single-pot, solid-phase-enhanced sample preparation for proteomics experiments. *Nat. Protoc.* **2019**, *14* (1), 68−85.
(35) Edwards, A.; Haas, W. Multiplexed Quantitative Proteomics for High-Throughput Comprehensive Proteome Comparisons of Human Cell Lines. *Methods Mol. Biol.* **2016**, *1394*, 1−13.
(36) Sive, H. L. *Xenopus: A Laboratory Manual*; Cold Spring Harbor Laboratory Press, 2023.
(37) Nieuwkoop, P. D.; Faber, J. *Normal Table of Xenopus laevis (Daudin): A Systematical and Chronological Survey of the Development from the Fertilized Egg Till the End of Metamorphosis*; Garland Publications, 1994.
(38) Mitulović, G.; Stingl, C.; Steinmacher, I.; Hudecz, O.; Hutchins, J. R.; Peters, J. M.; Mechtler, K. Preventing carryover of peptides and proteins in nano LC-MS separations. *Anal. Chem.* **2009**, *81* (14), 5955−5960.

https://doi.org/10.1021/acs.jproteome.5c00356
J. Proteome Res. XXXX, XXX, XXX−XXX

(39) Zahn, N.; James-Zorn, C.; Ponferrada, V. G.; Adams, D. S.; Grzymkowski, J.; Buchholz, D. R.; Nascone-Yoder, N. M.; Horb, M.; Moody, S. A.; Vize, P. D.; Zorn, A. M. Normal Table of Xenopus development: a new graphical resource. *Development* **2022**, *149* (14), No. dev200356, DOI: 10.1242/dev.200356.
(40) Wühr, M.; Freeman, R. M., Jr.; Presler, M.; Horb, M. E.; Peshkin, L.; Gygi, S.; Kirschner, M. W. Deep proteomics of the Xenopus laevis egg using an mRNA-derived reference database. *Curr. Biol.* **2014**, *24* (13), 1467−1475.
(41) Peshkin, L.; Gupta, M.; Ryazanova, L.; Wuhr, M. Bayesian Confidence Intervals for Multiplexed Proteomics Integrate Ion-statistics with Peptide Quantification Concordance. *Mol. Cell Proteomics* **2019**, *18* (10), 2108−2120.
(42) Shannon, A. E.; Teodorescu, R. N.; Soon, N.; Heil, L. R.; Jacob, C. C.; Remes, P. M.; Rubinstein, M. P.; Searle, B. C.A workflow for targeted proteomics assay development using a versatile linear ion trap, 2024. DOI: 10.1101/2024.05.31.596891.
(43) Huttlin, E. L.; Jedrychowski, M. P.; Elias, J. E.; Goswami, T.; Rad, R.; Beausoleil, S. A.; Villen, J.; Haas, W.; Sowa, M. E.; Gygi, S. P. A tissue-specific atlas of mouse protein phosphorylation and expression. *Cell* **2010**, *143* (7), 1174−1189.
(44) The, M.; MacCoss, M. J.; Noble, W. S.; Kall, L. Fast and Accurate Protein False Discovery Rates on Large-Scale Proteomics Data Sets with Percolator 3.0. *J. Am. Soc. Mass Spectrom.* **2016**, *27* (11), 1719−1727.
(45) Makarov, A. Electrostatic axially harmonic orbital trapping: a high-performance technique of mass analysis. *Anal. Chem.* **2000**, *72* (6), 1156−1162.
(46) Hu, Q.; Noll, R. J.; Li, H.; Makarov, A.; Hardman, M.; Graham Cooks, R. The Orbitrap: a new mass spectrometer. *J. Mass Spectrom* **2005**, *40* (4), 430−443.
(47) Schwartz, J. C.; Senko, M. W.; Syka, J. E. A two-dimensional quadrupole ion trap mass spectrometer. *J. Am. Soc. Mass Spectrom.* **2002**, *13* (6), 659−669.
(48) Peshkin, L.; Wuhr, M.; Pearl, E.; Haas, W.; Freeman, R. M., Jr.; Gerhart, J. C.; Klein, A. M.; Horb, M.; Gygi, S. P.; Kirschner, M. W. On the Relationship of Protein and mRNA Dynamics in Vertebrate Embryonic Development. *Dev. Cell* **2015**, *35* (3), 383−394.
(49) Nusinow, D. P.; Szpyt, J.; Ghandi, M.; Rose, C. M.; McDonald, E. R., 3rd; Kalocsay, M.; Jane-Valbuena, J.; Gelfand, E.; Schweppe, D. K.; Jedrychowski, M.; et al. Quantitative Proteomics of the Cancer Cell Line Encyclopedia. *Cell* **2020**, *180* (2), 387−402.
(50) Fang, P.; Ji, Y.; Silbern, I.; Doebele, C.; Ninov, M.; Lenz, C.; Oellerich, T.; Pan, K. T.; Urlaub, H. A streamlined pipeline for multiplexed quantitative site-specific N-glycoproteomics. *Nat. Commun.* **2020**, *11* (1), No. 5268.
(51) Udeshi, N. D.; Mani, D. C.; Satpathy, S.; Fereshetian, S.; Gasser, J. A.; Svinkina, T.; Olive, M. E.; Ebert, B. L.; Mertins, P.; Carr, S. A. Rapid and deep-scale ubiquitylation profiling for biology and translational research. *Nat. Commun.* **2020**, *11* (1), No. 359.
(52) Nguyen, T.; Costa, E. J.; Deibert, T.; Reyes, J.; Keber, F. C.; Tomschik, M.; Stadlmeier, M.; Gupta, M.; Kumar, C. K.; Cruz, E. R.; et al. Differential nuclear import sets the timing of protein access to the embryonic genome. *Nat. Commun.* **2022**, *13* (1), No. 5887.
(53) Shen, Y.; Dinh, H. V.; Cruz, E. R.; Chen, Z.; Bartman, C. R.; Xiao, T.; Call, C. M.; Ryseck, R. P.; Pratas, J.; Weilandt, D.; et al. Mitochondrial ATP generation is more proteome efficient than glycolysis. *Nat. Chem. Biol.* **2024**, *20* (9), 1123−1132.
(54) Reinecke, M.; Brear, P.; Vornholz, L.; Berger, B. T.; Seefried, F.; Wilhelm, S.; Samaras, P.; Gyenis, L.; Litchfield, D. W.; Medard, G.; et al. Chemical proteomics reveals the target landscape of 1,000 kinase inhibitors. *Nat. Chem. Biol.* **2024**, *20* (5), 577−585.
(55) He, Y.; Shishkova, E.; Peters-Clarke, T. M.; Brademan, D. R.; Westphall, M. S.; Bergen, D.; Huang, J.; Huguet, R.; Senko, M. W.; Zabrouskov, V.; et al. Evaluation of the Orbitrap Ascend Tribrid Mass Spectrometer for Shotgun Proteomics. *Anal. Chem.* **2023**, *95* (28), 10655−10663.
(56) Baxi, A. B.; Li, J.; Quach, V. M.; Pade, L. R.; Moody, S. A.; Nemes, P. Cell lineage-guided mass spectrometry reveals increased energy metabolism and reactive oxygen species in the vertebrate organizer. *Proc. Natl. Acad. Sci. U.S.A.* **2024**, *121* (6), No. e2311625121.
(57) Erickson, B. K.; Rose, C. M.; Braun, C. R.; Erickson, A. R.; Knott, J.; McAlister, G. C.; Wuhr, M.; Paulo, J. A.; Everley, R. A.; Gygi, S. P. A Strategy to Combine Sample Multiplexing with Targeted Proteomics Assays for High-Throughput Protein Signature Characterization. *Mol. Cell* **2017**, *65* (2), 361−370.
(58) Pekar Second, T.; Blethrow, J. D.; Schwartz, J. C.; Merrihew, G. E.; MacCoss, M. J.; Swaney, D. L.; Russell, J. D.; Coon, J. J.; Zabrouskov, V. Dual-pressure linear ion trap mass spectrometer improving the analysis of complex protein mixtures. *Anal. Chem.* **2009**, *81* (18), 7757−7765.
(59) Perez-Riverol, Y.; Bai, J.; Bandla, C.; Garcia-Seisdedos, D.; Hewapathirana, S.; Kamatchinathan, S.; Kundu, D. J.; Prakash, A.; Frericks-Zipper, A.; Eisenacher, M.; et al. The PRIDE database resources in 2022: a hub for mass spectrometry-based proteomics evidences. *Nucleic Acids Res.* **2022**, *50* (D1), D543−D552.

https://doi.org/10.1021/acs.jproteome.5c00356
J. Proteome Res. XXXX, XXX, XXX−XXX